

Evaluation of Disbondings and Measurement of Poisson's Ratio for Plastic Composites Using Holographic Interferometry

MASAKI KIMOTO, ITSUO NAGATA, AKIO MINOWA,
KOUSUKE MORIWAKI, and TOSHIAKI WATANABE, *Osaka
Prefectural Industrial Technology, Research Institute,
Higashi-Osaka, 577 Japan*

Synopsis

Disbondings and Poisson's ratio were examined for several plastics composite plates using holographic interferometry. The displacement at the disbondings could be detected below submicrometer order. The value of Poisson's ratio strongly depended upon orientation and type of fiber and laminate construction.

INTRODUCTION

It is relatively easy to prepare fiber-reinforced plastics (FRP) with desired chemical and mechanical properties by selecting resin, type of fiber, construction of laminate, etc., and by avoiding serious defects on molding. This is one of the most convenient advantages of FRP, and, for this reason, all kinds of FRP are utilized in a wide variety of industry.

Analysis of the relationship between FRP structure and its mechanical properties has been extensively studied. However, little has been reported on the relation between the construction and the Poisson's ratio (ν) of FRP, which is an essential value for the analysis of deformation and vibration using the finite element method. Strain gage is widely used to measure ν . However, it is somewhat troublesome, and errors are caused by unevenness of the sample surface, alignment of the gage, and lack of adhesiveness to the sample.

Serious defects caused on molding might affect the mechanical properties of FRP in some case, and sometimes desired characteristics are not attained. These defects must be detected before use. In addition, it is necessary that the FRP plates be tested without destruction as to whether they possess the characteristics as designed.

Holographic interferometry is one of the most useful testing methods by nondestruction both for detecting possible failures and for evaluating mechanical properties. Application of this method to the testing of FRP has already been reported.^{1,2} However, these studies were concerned only with detection of disbondings, and little has been studied about quantitative treatment. Earlier workers proposed the use of the holographic technique for the measurement of ν .³ Recently, by the use of this method, ν for orthotropic FRP has been determined and suitability of the application has been examined.⁴

In this study, the lower limit of pore size detected and the displacement of skin layer under reduced pressure were examined for an FRP plate using the holographic method. Also ν was measured for several FRP laminates, and the effect of orientation and type of fiber and construction of laminate were discussed.

EXPERIMENTAL

Materials

FRP plates were prepared by press molding of prepreg (three types) or by hand-layup method (sandwich FRP; nine types). The prepreps used were glass fiber (GF) woven cloth/epoxy (EPC-160EPP) and carbon fiber (CF) woven cloth/epoxy (CFP-1122PP) (Arisawa Seisakusyo Co.). The epoxy resin used in the prepreg was a mixture of Epikote 828 and Epikote 1001 (Yuka-shell Epoxy Co.) with dicyan diamide hardener. The prepreg sheet was cut off in 0° or $+45^\circ$ orientation to the aligned lengthwise fiber direction. The specimen used for the evaluation of disbondings were shown in Figure 1. Twelve plies of 0° oriented sheets (12×25 cm) were laid up and pressed. Circular pores of five different sizes were machined, and two plies of 0° sheets (skin) were laid up on both sides of the machined plate and again pressed.

For the measurement of ν , cutoff prepreg sheets were laid up in two different manners (Fig. 2): laminate of 15 plies of 0° oriented sheets (A-type; GF-A, CF-A) and alternate lamination of 15 plies of 0° and 45° sheets (B-type; GF-B). The press condition was 130°C for 30 min at contact pressure. Fiber content of each plate was ~ 60 wt %. The thickness of each plate was ~ 2.5 mm.

Materials used for sandwich type FRP (C-type) are shown in Table I. The construction of the laminate is shown in Figure 2. Epoxy resin used for C-type was a mixture of Epikote 828 and B-002W (Yuka-shell Epoxy Co.) (100 : 60). Neat epoxy plate was also prepared from this mixture. C-type FRP and neat epoxy plates were cured at room temperature for 24 h and at 60°C for 3 h. The thickness of C-type FRP plates was in the range of 2.1–3.7 mm. Prepared plates were machined in 0° – 90° to the lengthwise fiber direction of surface layer (only 0° for C-type) into a size of 50×180 mm.

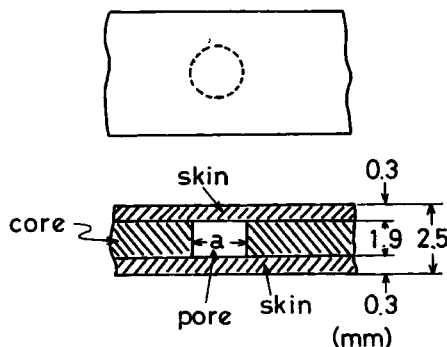


Fig. 1. The specimen used for the evaluation of disbondings. ($a = 5.0, 4.0, 3.5, 3.0, 2.5$ mm.)

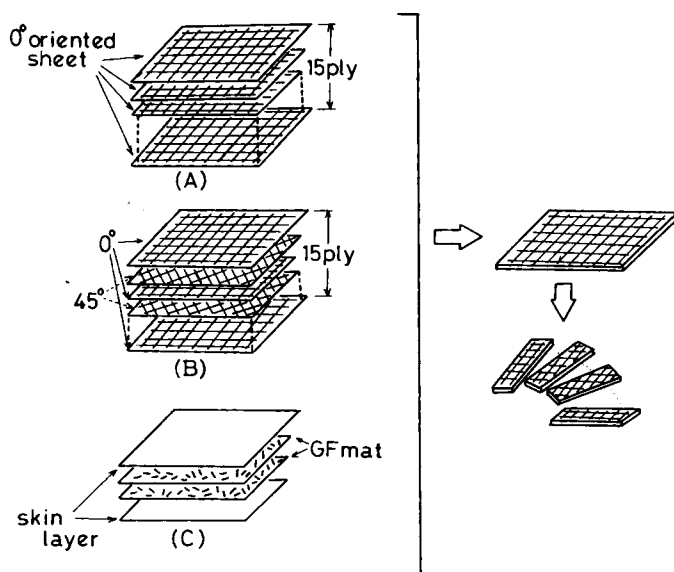


Fig. 2. The procedure to prepare specimen for the measurement of ν . [Cutoff plates in a certain angle were abbreviated as, for example, GF-B (90°).]

TABLE I
Materials Used for C-Type FRP and ν for FRP Plate

| | Reinforcement used for skin layer | Weight per unit area of the skin (g/m ²) | Fiber content of FRP plate (vol %) | ν for FRP plate |
|-----|--|--|--|------------------------|
| C-1 | CF cloth Torayca #6341 | 400 | 23.6 | 0.091 |
| C-2 | CF cloth Torayca #6343 | 200 | 24.5 | 0.124 |
| C-3 | KF ^a cloth Kanebo K281 | 170 | 26.1 | 0.115 |
| C-4 | CF-KF hybrid cloth ^b Kanebo CK3104 | 173 | 26.0 | 0.103 |
| C-5 | CF-KF hybrid cloth ^b Kanebo CK3102 | 181 | 24.1 | 0.088 |
| C-6 | GF cloth Nittobo WF-350 | 350 | 23.7 | 0.151 |
| C-7 | GF cloth Nippon Sheet Glass YES-2101 | 305 | 23.1 | 0.172 |
| C-8 | GF cloth Nippon Sheet Glass YEH-1001 | 93.6 | 22.6 | 0.238 |
| C-9 | GF mat Nippon Sheet Glass REW-300G5 | 300 | 18.4 | 0.366 |

^aKF = Kevlar fiber.

^bCF-KF hybrid cloth, CK3104 and CK3102, contain KF and CF 2 : 1, and 1 : 1 in volume ratio, respectively.

^cReinforcement used for the core; GF mat REW-450G5 (450 g/m²; Nippon Sheet Glass).

Measurement

Figure 3 shows the schematic of experimental setup. Holographic system (Fuji Photo Optical Co.) has a 5-W argon-ion laser (Model 2025-05, Spectra Physics Co.) as a light source. A collimated beam of the laser was divided into two beams by a beam splitter. The reflected beam illuminated the surface of the test piece and the scattered light fell on a hologram plate. The transmitted beam, on the other hand, was reflected by a mirror and brought as a reference beam onto the hologram plate and interfered with the object beam. After the hologram was made using a holographic camera, a set of real time displacement fringes was induced by mechanically deforming the test piece. The test piece supported by a pair of steel rods (150 mm distance) was loaded through another pair (80 mm distance) on the back surface. Vacuum vessel was also used if necessary. When the processed holographic plate was viewed against the reference beam, it reconstructed the image of the object with a fringe pattern related to the displacement. The holographic fringes were imaged by a video camera placed at the back of a hologram plate and a TV monitor.

The principle of measurement of ν is as follows: The theory of elasticity in three dimensions gives the displacement of a isotropic plate surface after pure bending as⁵

$$u = [x^2 - \nu(y^2 + d^2)]/2R + \text{const} \quad (1)$$

where the xy -plane is defined as the plate surface, the bending load is along the z -axis, R is the radius of curvature of the plate after bending, and $2d$ is the plate thickness. The contour lines of the surface displacements are hyperbolas with the asymptotes

$$x^2 - \nu y^2 = 0 \quad (2)$$

and the smaller angle 2α between them is related to ν ,

$$\nu = \tan^2 \alpha \quad (3)$$

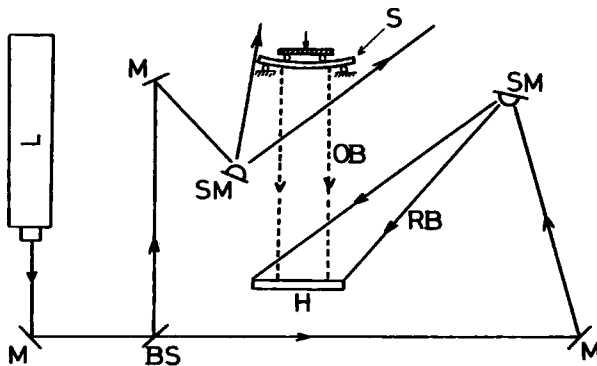


Fig. 3. The schematic of experimental setup. (L) laser; (M) mirror; (BS) beam splitter; (SM) spherical mirror; (S) specimen; (OB) object beam; (RB) reference beam; (H) hologram.

The contour lines can be obtained by the interferometric methods. Therefore, the determination of ν only involves the measurement of the angle 2α between two asymptotes of the displacement pattern of the test specimen for every loading condition. Figure 4 shows an example of interferogram for a GF-B (90°) plate in bending. The angle between the asymptotes of the hyperbolas were measured for two to four loading conditions and the average

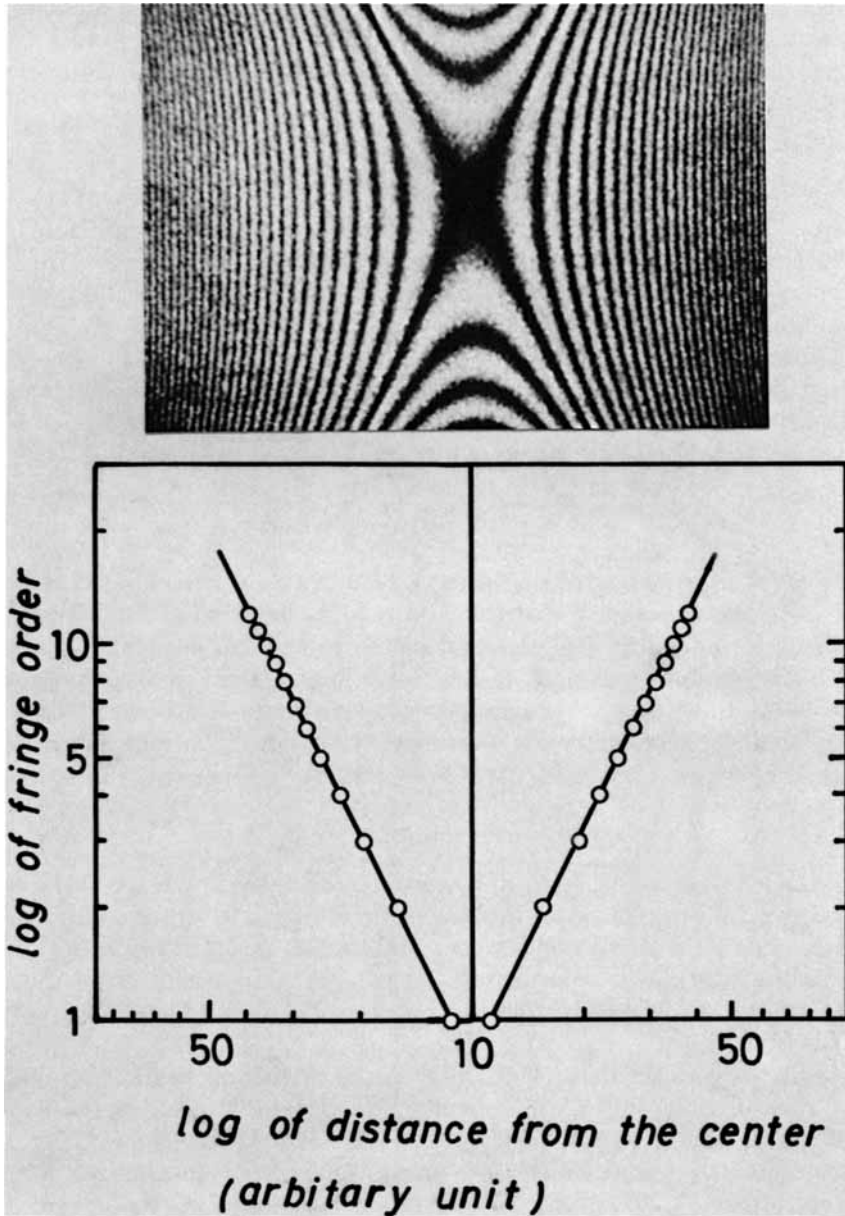


Fig. 4. Interferograms for GF-B (90°) and logarithmic plot of fringe order against the distance from the center along x -axis.

value was employed. Using the real time method, it was possible to adjust asymmetry of fringes caused by a small tilt of the plate.

RESULTS AND DISCUSSION

Evaluation of Disbondings in FRP

Figure 5 shows the interferogram obtained for the FRP plate with pores under reduced pressure. The disbonding area was easily observed with a small fringe. Air included in the pore would expand under reduced pressure and cause displacement of the skin FRP. The distance between two fringes correspond to half a wavelength of the laser light used, and accordingly the displacement could be estimated from the fringe order, namely,¹

$$d = n \cdot \lambda / 2 \quad (4)$$

where n is a fringe order, λ is the wavelength ($0.5145 \mu\text{m}$). From Figure 5, the deviation in the fringe pattern was 1 fringe for 3.5-mm pore and 1/2 fringe for 3-mm pore. Therefore, the displacement of the skin FRP at the pore was calculated to be 0.26 and $0.13 \mu\text{m}$, respectively. On the other hand, the displacement can be estimated by simple material mechanics. For the pore it should be assumed that the skin FRP was fixed at circumference and the pressure was loaded uniformly. The maximum displacement at the center of the skin FRP, W_{max} , was calculated by the following equation⁶:

$$W_{\text{max}} = 0.171 \cdot P \cdot r^4 / E \cdot h^3 \quad (5)$$

where P = pressure load at unit area ($1 \times 10^5 \text{ Pa}$), r = the radius of the pore, E = elastic modulus ($2 \times 10^{10} \text{ Pa}$), and h = thickness of the skin FRP ($3 \times 10^{-4} \text{ m}$). From eq. (5), W_{max} was calculated to be $0.297 \mu\text{m}$ for 3.5-mm pore, and $0.129 \mu\text{m}$ for 3-mm pore, respectively. These values were in good agreement with the holographic data. From these results, it is concluded that holographic interferometry could estimate the displacement of submicrometer order.

Measurement of ν for FRP

In the lower graph of Figure 4, fringe order along the x -axis for both the left and right side was plotted against the distance from the center on logarithmic scales. The slopes of both lines were equal to 2 as expected from eq. (1). This proves that the elastic deformation can be approximated for the orthotropic plate under small deformation, and this method can be applied for the measurement of ν .

Figure 6 shows the dependence of ν on the cutting off angle (fiber orientation) measured for CF-A, GF-A, and GF-B. Obtained ν were quite large at $\sim 45^\circ$, and quite small at $\sim 0^\circ$ and $\sim 90^\circ$. It has been known that FRP takes quite large (above unity) or small values (zero or negative values)⁷; however, there have not been sufficient investigations on these anomalous values, except for the recent theoretical study by Miki.⁸ Apparent from the results, the deviation in ν was larger for A type than for B. This should be due

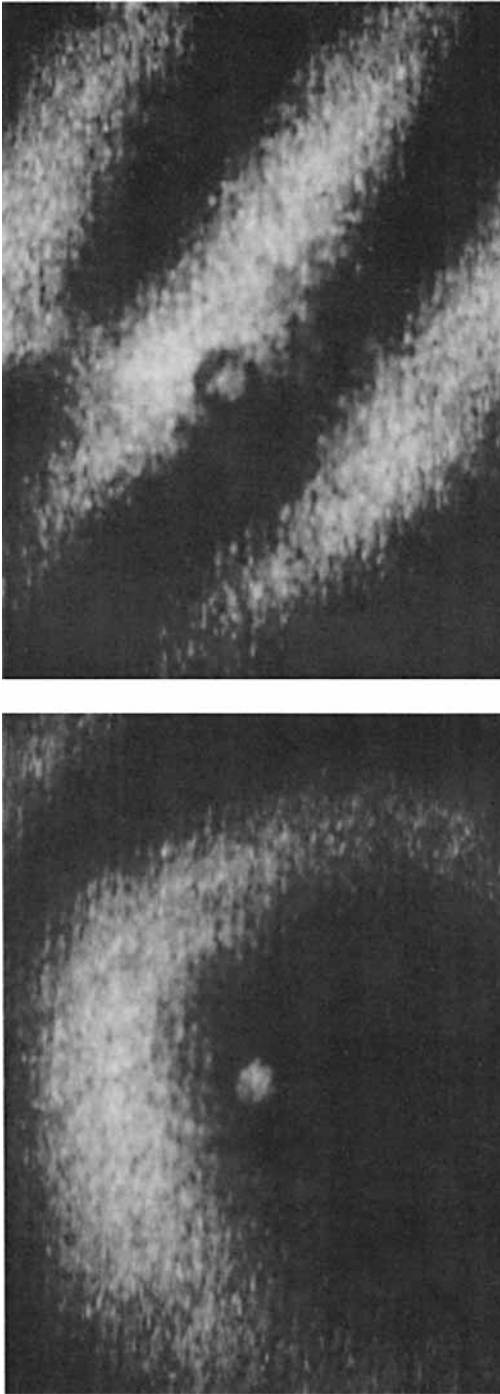


Fig. 5. Interferograms for the FRP plate including pores under reduced pressure: (left) 3.0 mm; (right) 3.5 mm.

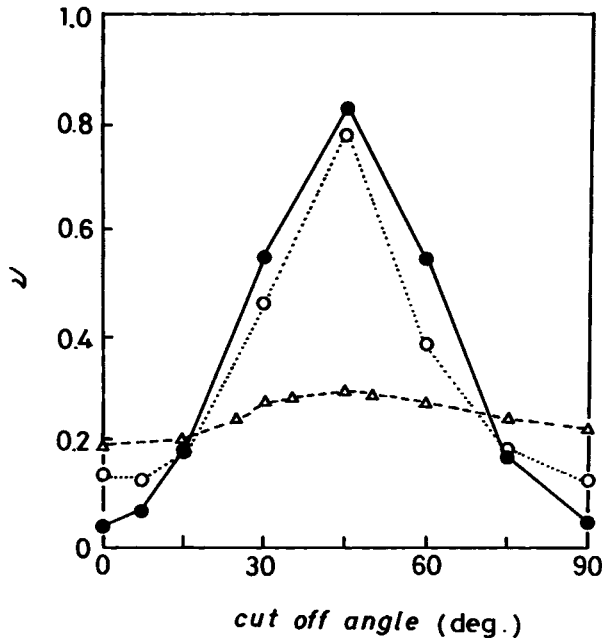


Fig. 6. The dependence of ν on cutting off angle (fiber orientation): (—●—) CF-A; (···○···) GF-A; (---△---) GF-B.

to the difference in laminate construction; A-type FRP, which were laid up all sheets in the same orientation, should have larger directional dependence of mechanical characteristics compared with B type, which consisted of 0° and alternative 45° layers. The larger deviation in ν for CF-A compared with GF-A should be related to the larger differences in modulus for CF-A between horizontal and vertical directions.

Table I shows the measured ν for C-type FRP (0° direction). ν obtained for the neat epoxy resin was 0.39, which was in good agreement with the literature.^{4,9} ν 's of GF have been reported to be ~ 0.20 .^{4,9} Glass mat has no directionality; therefore, C-9 would be expected to have the intermediate ν value between those of neat epoxy and GF. The ν obtained was of intermediate value as expected. Quite small values were obtained for other laminates. All of them were larger in fiber contents compared with C-9, and contained directional cloths in skin layers. Rao et al. reported the dependence of ν on fiber content for a glass woven cloths FRP.⁴ Considered from their results, the difference in the fiber content must not have so much an effect in our case (less than 10%). On the other hand, as in Figure 6, the difference in laminate construction and fiber orientation should affect the ν value. Small ν could be attributed to 0° oriented skin layer. For three types of FRP with GF woven cloths skin layer (C-6, C-7, and C-8), there was a tendency that the laminate with thin skin layer (light weight per unit area) showed larger ν compared with the thick skin laminates. Thick cloths might have an effect with large directionality. There was a similar tendency for CF woven cloths. There were small differences in ν between the laminates with CF, KF, or CF-KF hybrid

cloths for skin layer. Much detailed examination, both experimental and theoretical, are required to discuss these small differences.

CONCLUSIONS

Holographic interferometry could estimate the displacement at disbondings in FRP below submicrometer order. The values of Poisson's ratio for several FRP plates were also measured by using the holographic method. The values strongly depended upon fiber orientation, type of fiber, and laminate construction. These results would present considerable significance for composite designers.

We wish to express our sincere thanks to Dr. Toshikazu Misaki and Dr. Kiyoshi Mizutani of Osaka Prefectural Industrial Technology Research Institute for the helpful discussion and encouragement.

References

1. T. Winkler, F. E. Jesnitzer, and H. Haferkamp, 36th Annual Conference, Reinforced Plastics/Composites Institute, The Society of the Plastic Industry, Session 10-E, 1981.
2. T. Hosokawa and M. Hosoya, *Jpn. J. Compos. Mater.*, **10**, 122 (1984).
3. I. Yamaguchi and H. Saito, *Jpn. J. Appl. Phys.*, **8**, 768 (1969).
4. R. M. V. G. K. Rao, M. Swaminadham, and K. Rajanna, *Fiber Sci. Technol.*, **15**, 235 (1981).
5. S. Timoshenko and J. N. Goodier, *Theory of Elasticity* 2nd ed., McGraw-Hill, New York, 1951, p. 250.
6. *Kikai-Kogaku Binran*, 4th ed., The Japan Society of Mechanical Engineers, Tokyo, 1960, pp. 4-55.
7. S. W. Tsai and H. T. Hahn, *Introduction to Composite Materials*, Technomic, Lancaster, PA, 1980, p. 156.
8. M. Miki, private communication.
9. D. Hull, *An Introduction to Composite Materials*, Cambridge University Press, Cambridge, 1982, p. 27.

Received April 12, 1989

Accepted April 14, 1989